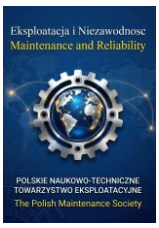

Eksploatacja i Niezawodnosc - Maintenance and Reliability

Volume 29 (2027), Issue 1

https://ein.org.pl

The Polish Maintenance Society

A PSO-HMM-based intelligent defect identification method for power grid security and stability control system

Yu Chen[1,*], Hang Jiang[1], Qiang Lan[1], Haoyu Wang[1]

[1] Southwest Branch of State Grid Corporation of China, China
* Corresponding Author: yuchen070180@163.com

Received: 24 April 2026
Revised: 4 May 2026
Accepted: 9 May 2026
Online: 9 July 2026

Abstract

The security and stability control system (SSCS), as the second line of defense for power grid security, relies primarily on manual judgment for defect identification currently, which suffers from low efficiency and limited accuracy. Traditional methods are restricted by local optimization during training, while the complex inter-device coupling and scarce historical defect data of SSCS further hinder effective defect identification. Therefore, an SSCS defect identification method based on Particle Swarm Optimization and Hidden Markov Model (PSO-HMM) is proposed. First, SSCS defects are sorted and classified into 5 categories, and 10 key characteristic quantities are mined to characterize SSCS operational states. To overcome the local optimization problem, the PSO algorithm is introduced to optimize the initial observation probability matrix of HMM, and a PSO-HMM-based SSCS defect identification model is established. The model is validated using 2500 defect samples collected from a regional power grid SSCS. Results show that the proposed method enables accurate real-time identification of SSCS defects, provides a scientific basis for SSCS condition-based maintenance.

Keywords: *power system, safety and stability control system, identification model, hidden Markov model, defect feature quantity*

Article citation:
Chen Y, Jiang H, Lan Q, Wang H, A PSO-HMM-based intelligent defect identification method for power grid security and stability control system, Eksploatacja i Niezawodnosc – Maintenance and Reliability 2027: 29(1) http://doi.org/10.17531/ein/221636

Highlights

- Optimizing HMM to solve the local optimization problem in SSCS defect data training.
- Constructing a dedicated SSCS defect feature system.
- Realizing in-depth adaptation between the defect identification method and the traits.

1. Introduction

To address the spatial mismatch between load and energy centers, interconnections among regional power grids and long-distance transmission projects have been continuously developed [1,2]. However, the stability of the large-scale power grid has been increasingly challenged. In addition to ensuring sufficient static stability reserves and power backup capacity, it is necessary to design control measures to respond to potential fault conditions. Power grid has established a three-level security and stability criterion along with a three-tier defense system. The security and stability control system (SSCS), constructed according to the second-level stability criterion, serves as the second defense line [3–5]. It primarily targets system faults and executes actions such as generator tripping, load shedding, and regional separation in accordance with predefined control strategies to prevent system instability. In AC/DC interconnected power systems, the scope of fault propagation has significantly expanded. Implementing multi-measure, wide-area, and fine-grained regulation through the SSCS, and effectively preventing incidents that cause abnormal SSCS operation, have become major challenges for maintaining grid stability [6].

With the large-scale integration of renewable energy sources and the resulting changes in power grid structure, the deployment configuration and control strategies of the SSCS should be further improved. The operational state of the SSCS is influenced not only by the devices within its own region but also by those in interconnected areas. Minor device faults may be amplified through communication links, causing cascading interactions across regions. Consequently, the operational state

of the SSCS depends on both local and associated plant conditions. The SSCS operates only during grid faults and remains in a networked standby state at other times, except during maintenance. Therefore, in addition to real-time monitoring, identifying the SSCS operational state based on long-term operational data has become an effective supplementary approach to ensuring the reliability of power grid operation. However, the defect identification of the SSCS still primarily depends on manual judgment based on operational experience. This manual process suffers from inefficiency and limited accuracy, which severely threatens the reliability of the SSCS and the security and stability of the power grid [7]. Thus, establishing an intelligent and quantitative defect identification method is an urgent requirement.

Several studies have been conducted on the identification of defects in power equipment. The mathematical models are used to extract the fault information for defect identification. However, the mathematical model of SSCS could not be established due to the complex structure and interconnections. Signal processing methods are adopted to identify defects by analyzing the signal characteristics. However, SSCS has diverse types of state signals that interfere with each other. Expert system methods can establish association rules between alarm information and identify defects based on historical databases. However, there are limited historical defect data for SSCS, and the association rules could not be established because of the complex logic functions of SSCS. Moreover, the existing defect identification methods are primarily designed for primary equipment. These methods cannot be directly applied to SSCS because the composition and operating principles of SSCS are different.

Some researches focus on the defect identification of relay protection devices. The association between protection device defects and alarm information is mined via an association rules algorithm, and a defect identification method of protection device based on a relational hypergraph enhanced Transformer is proposed [8]. A fault diagnosis model for a protection device is established by introducing the generalized transformation ratio of the measurement circuit [9]. An improved PSO-optimized SVM algorithm is used to build a fault diagnosis model [10]. There are some similarities between the SSCS and the protection device, but the architecture, configuration, operation principles, and functions are different. Besides, existing defect identification methods mainly target individual components or devices without fully considering the inter-device associations. Therefore, the existing methods are hard to apply to SSCS.

In recent years, substantial scholarly attention has been directed toward the online status evaluation of SSCS. For instance, a dynamic reliability evaluation framework utilizing Markov Chain Monte Carlo was developed in [11], while [12] established a hierarchical evaluation index system based on membership weighted calculations. However, these methodologies predominantly rely on fuzzy set theory and comprehensive evaluation, which are often constrained by a heavy dependence on expert heuristics and exhibit limited efficacy in capturing the dynamic evolution inherent in massive time-series data. Parallel efforts in SSCS defect identification have yielded significant insights. Researchers have summarized potential hidden faults and established overarching reliability frameworks [13,14]. Specific technical approaches include the cross-verification of homologous analog quantities [15], defect correlation analysis via improved Apriori algorithms [16], and fault diagnosis through digital twin integration [17]. Recently, deep belief networks (DBN) have been introduced for automated diagnosis [18]. Nevertheless, the deployment of such deep learning architectures is frequently hampered by their stringent requirements for sample size and data quality. Given the high reliability of SSCS, historical defect data remain relatively scarce and characterized by progressive temporal evolution, thereby restricting the practical engineering applicability of purely data-driven methods.

The SSCS features a complex structure with strong coupling relationships among its devices, making it challenging to accurately develop a defect identification model. Moreover, the SSCS operates under nearly constant conditions for extended periods, with limited data variation and numerous monitoring variables. Therefore, this study proposes an SSCS defect identification method based on the fusion of PSO and Hidden Markov Model (PSO-HMM), with three key innovations: (1) Developed a hybrid identification model utilizing Particle Swarm Optimization to overcome the local optima of traditional HMMs, significantly enhancing training stability and identification accuracy; (2) Constructed a multi-dimensional

characteristic system comprising 10 key indicators across temporal, operational, sampling, and power domains to achieve high-fidelity state characterization; (3) Achieved deep adaptation of the identification method to address the challenges of strong inter-device coupling and scarce historical data, ensuring robust engineering applicability for regional power grids.

This paper is organized as follows: First, the types and causes of defects in various stages of the SSCS were analyzed, and key features characterizing its operational states were extracted. Then, the PSO algorithm was incorporated into the HMM parameter training process. Accordingly, a PSO–HMM-based defect identification model for the SSCS was developed, from which the SSCS defect identification method was proposed. Finally, historical defect samples from the SSCS were employed to verify the validity and effectiveness of the proposed method.

2. Defects and characteristic quantity of SSCS

The architecture of a SSCS is typically classified into three categories: local, regional, and hy-brid [17]. A local SSCS is independently deployed within substations or power plants to rapidly mitigate stability risks—such as busbar, main transformer, or outgoing line faults—without re-quiring cross-station communication. In contrast, a regional SSCS utilizes a hierarchical frame-work comprising a master station, substations, and execution units; it maintains wide-area stability through centralized fault data processing and strategy decision-making at the master level. As shown in Fig. 1, the hybrid architecture integrates features of both, where the master station con-solidates global operational status and identifies operation modes while disseminating critical data to substations to facilitate autonomous local response. Driven by large-scale renewable en-ergy integration and grid interconnections, the development of modern power systems is trending toward collaborative defense and resource optimization through dedicated multi-regional infor-mation channels.

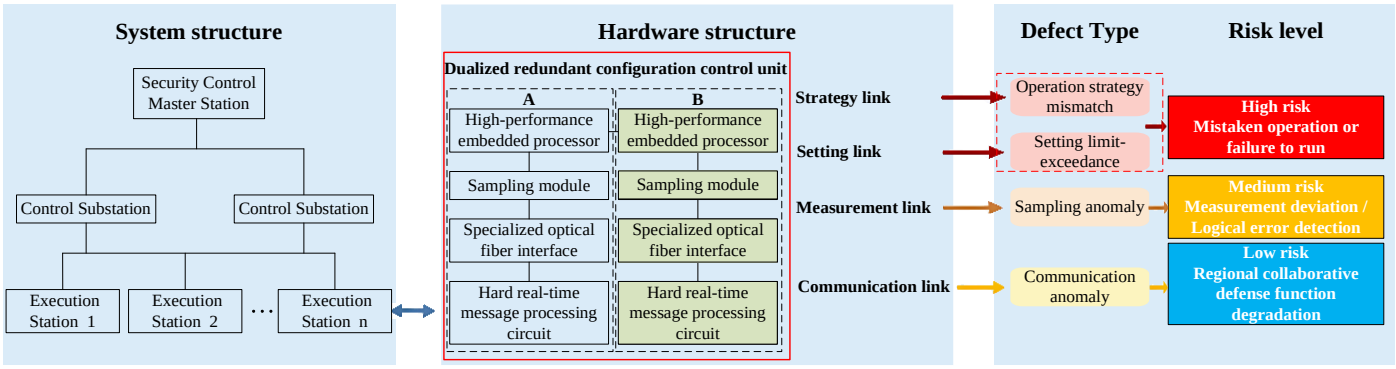

Figure 1. Structure composition of SSCS.

SSCS hardware generally adopts a dual-redundant configuration (A/B systems) to ensure ex-treme operational reliability. The core computing platform integrates high-performance mul-ti-core processors (CPU/DSP) and large-scale Field Programmable Gate Arrays (FPGA) to support complex transient stability calculations and real-time security control logic. At the interface level, the device captures electrical signals, including current and voltage, via high-precision analog sampling modules. Simultaneously, optoisolated I/O modules are utilized to monitor real-time circuit breaker statuses and execute critical trip commands, such as generator tripping and load shedding. Regarding communication, the system is equipped with dedicated fiber-optic interfaces and hard real-time message processing circuits, ensuring deterministic data transmission and low-latency interaction between stations. Furthermore, internal self-checking and auxiliary sens-ing circuits are integrated to monitor board temperature, humidity, power supply status, and logic matching values in real-time, with all data consolidated via a centralized monitoring platform for condition-based assessment.

The SSCS adopts decentralized control and information processing, so its defects are distributed and may appear in multiple links, including strategy, voting mode, software, communication, measurement, setting, and manual operation [19]. The strategy link of SSCS compares the signals from the measurement link with the standards set by the setting link. There may be mismatches between the actual grid operation mode and the strategy, which can cause the SSCS to

malfunction or fail to operate [16]. Software link defects primarily include software logic errors, program design errors, and protection setting errors, which typically manifest as internal logic state anomalies. The operational information for these defects is predominantly reflected in system event records and operation logs. Most software link defects can be recorded and uploaded as alarms through the SSCS security information and event management system, which captures abnormal logic states and operation logs during the software execution process. Furthermore, during regular offline logic verification and protection setting debugging, operation and maintenance personnel can utilize dedicated test software provided by the manufacturer for identification and troubleshooting. The voting mode link utilizes a redundant design method to improve SSCS security, effectively preventing failures to operate or maloperations caused by hidden faults in a single set of device. Anomalies in the voting mode link do not directly cause a failure to operate or maloperation of the SSCS; instead, they are mainly identified and investigated through the multi-channel data consistency comparison logic designed inside the device or during planned offline maintenance. Consequently, discovering defects within both the software link and the voting mode link relies heavily on the manufacturer's dedicated test software or periodic offline maintenance

The communication link may experience data loss, high bit-error rates, signal interruptions, or transmission errors, which can lead to communication failure and affect command reception and execution. The measurement link uses current and voltage transformers to collect signals. Its defects include out-of-bound sampling values and significant deviations in measured system values [18]. The setting link directly determines whether the SSCS can respond correctly. Its defects are usually manifested as setting limit-exceedances, configuration errors, and logic-judgment issues, which can prevent normal system operation and cause unintended actions or failures to operate. Operators' improper actions can also lead to system defects. Common human-induced operational faults involve configuration mistakes, improper debugging, or neglecting equipment maintenance. Therefore, the SSCS defect identification method proposed in this paper does not consider the software link and the voting mode link, and is divided into 5 categories according to the principles of external feature observability and data sample accessibility: normal, communication anomaly, sampling anomaly, setting limit-exceedance, and operation strategy mismatch.

In order to clarify the importance degree of different defects in the system operation, according to the actual hazard degree of the defects on the action behavior of the SSCS, risk level division and logical sorting are carried out for typical defects. The SSCS, as a functional system taking the control strategy as the core, its operational risk essentially depends on the influence degree of each functional link on the correctness of the device action. According to the actual hazard degree of different defects on the safe and stable operation of the system, typical defects can be divided into three categories: high risk, medium risk, and low risk. The first is high-risk defects (direct hazard), including operation strategy mismatch and setting limit-exceedance, such defects may directly lead to maloperation or failure to operate of the SSCS device; the second is medium-risk defects (data distortion), including sampling anomaly, such defects will cause electrical quantity measurement deviation, and then trigger protection logic misjudgment; the third is low-risk defects (function degradation), including communication anomaly, such defects mainly affect the real-time performance of data interaction, and may lead to the degradation of the regional cooperative defense function.

Using key characteristic quantities can reflect the operational status of SSCS. The operation status of SSCS includes the equipment operation status and the communication system status. The equipment operation status refers to whether the security control devices at each factory and substation are working normally. The communication system status involves the communication efficiency between dual-configured security control devices within the same site, as well as the communication accuracy and transmission speed between devices at different sites. Using the criteria of measurability, representativeness, ease of acquisition, and independence for screening, and based on the composition of the SSCS, the characteristics of device defects, and the requirements of grid regulations [18], this paper proposes ten key characteristic quantities to characterize the operation status of SSCS, as shown in Table 1. Time characteristic quantities reflect the communication system's operation status, including synchronization time differences and bit error rates. Operational

characteristic quantities indicate whether the working environment of security control devices meets standards, covering device temperature, humidity, matching logic values, and online verification of setting values and safety margin. Sampling characteristic quantities reflect the operation status of the SSCS's measurement link, including frequency measurement error and switch status acquisition accuracy. Power characteristic quantities show whether the SSCS's working power is normal, including DC circuit power and AC circuit power. Matching logic values are 1 when the system's operation strategy matches the grid's actual operation mode; otherwise, they are 0, triggering an alarm. The safety margin of online verified settings is calculated by comparing current settings with preset reference values. These key characteristic quantities fully characterize the security control system's communication, measurement, settings, and strategy links.

Table 1. Defect characteristic quantity of SSCS.

Feature quantity category	Key characteristic quantity
Time characteristic	Synchronization time difference、Bit error rate
Operating characteristics	Internal temperature of the device、Internal humidity of the device、Match logical values、Online verification of setting values and safety margin
Sampling characteristics	Frequency measurement error、Switch status acquisition accuracy
Power characteristics	DC circuit power、AC circuit power

Specifically, the key defect characteristic for the communication link of the SSCS is the formula for calculating the communication bit error rate:

$$W = \frac{Ne}{N} \times 100\% \tag{1}$$

where N represents the total number of transmitted binary symbols; Ne represents the number of bit errors.

The key defect characteristic quantity for the setpoint section of the SSCS and the formula for calculating the safety margin of online calibration are as follows:

$$M_i = \frac{I_i}{I_{iN}} \tag{2}$$

where I_i represents the current setpoint of the i-th SSCS device; I_{iN} represents the predefined reference value of the i-th SSCS device.

The defect characteristic quantity matching logic for the strategy section of the SSCS is as follows:

$$B = DO_i\overline{DO_N} + \overline{DO_i}DO_N \tag{3}$$

where DO_idenotes the operational strategy logic value that characterizes the actual operating mode of the power grid; DO_N denotes the operational strategy logic value that characterizes the operating strategy of the SSCS. When they match, B equals 0; when they do not match, B equals 1.

3. Defect identification model of SSCS based on PSO-HMM

Defects in SSCS are mostly unobservable and need to be inferred indirectly from measurable signals or indicators. As a probabilistic model for time series [19–21], HMM can reflect the varia-tion of defect characteristics in time series. The operation status of SSCS changes over time, and the state transition mechanism of HMM can capture the relationship between system operation status and observable data. HMM can adapt to the changing working conditions of SSCS. Espe-cially when there is a nonlinear relationship between defect characteristics and types, HMM can gradually improve the accuracy of defect identification through iterative learning. Therefore, this paper proposes a SSCS defect identification method based on HMM. First, extract and encode the defect characteristics of the SSCS. Then, establish a SSCS defect identification model using PSO and HMM. Finally, form observation vectors from preprocessed defect characteristics as inputs for model training.

The defect identification model of the SSCS based on HMM is shown in Fig. 2. It includes the initial probability matrix $\pi$of defect causes, the transition probability matrix $\boldsymbol{A}$ of defect causes, the observation probability matrix $\boldsymbol{B}$, the observation sequence $\boldsymbol{O}$, and the hidden sequence $\boldsymbol{S}$. We select N hidden states and M observation states. The dimension of the hidden state vector equals the number of defect causes, and the dimension of the observation vector equals the number of defect characteristics. The HMM model describing the statistical characteristics of the defect feature vector sequence of the SSCS can be described as follows:

$$\lambda = (\pi, A, B) \tag{4}$$

where the initial probability matrix π and transition probability matrix $\boldsymbol{A}$ determine the invisible defect cause state sequence. The observation probability matrix $\boldsymbol{B}$shows how these hidden states are transformed into observable

output sequences [21].

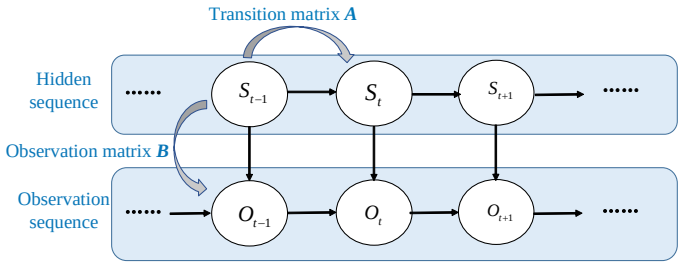

Figure 2. Defect identification model of SSCS based on HMM.

The initial probability matrix can be defined as: $\pi = (\pi_1, \pi_2, \ldots, \pi_N)$, it satisfies the following expressions:

$$\pi_i = P(o_0 = s_i) \tag{5}$$

where:

$$\sum_{i=1}^{K} \pi_i = 1 \tag{6}$$

The transition probability matrix can be defined as: $A = (a_{ij})_{N\times N}$, it satisfies the following expressions:

$$a_{ij} = P(i_{t+1} = s_j | i_t = s_i) \tag{7}$$

where $i = 1,2,\ldots,N; j = 1,2,\ldots,N$, a_{ij} can be denoted the probability of transitioning from defect state s_i at time t to defect state s_j at time t+1.

The observation probability matrix can be defined as: $B = (b_{ji})_{N\times M}$, it satisfies the following expressions:

$$b_j(o_i) = P(v_t = o_i | i_t = s_j) \tag{8}$$

where the probability of observing o_i at time t given defect state s_j is denoted by $b_j(o_i)$.

Model training aims to maximize the probability $P(O|\lambda)$ by using the Baum-Welch algorithm to find optimal model parameters λ, given the observation sequence $\boldsymbol{O}$ and initial probability matrix $\boldsymbol{\pi}$.

The Baum-Welch algorithm is a specific case of the Expectation-Maximization (EM) algorithm. Each iteration consists of two steps: the E-step to compute the expectation and the M-step to maximize the likelihood. The formula is as follows:

$$\lambda^{(t+1)} = \underset{\lambda}{argmax} \sum_{S}^{\sum^{(t)}} logP(O,S|\lambda)P(O,S|\lambda^{(t)}) \tag{9}$$

For the E-step, define:

$$Q(\lambda,\lambda^{(t)}) = \sum_{S}^{\sum^{(t)}} logP(O,S|\lambda)P(O,S|\lambda^{(t)}) \tag{10}$$

where $\lambda^{(t)} = (\pi^{(t)}, A^{(t)}, B^{(t)})$ is the estimated value of the HMM parameters at the current time step.

Substituting the parameters of the initial probability matrix π, the state transition probability matrix $\boldsymbol{A}$, and the observation probability matrix $\boldsymbol{B}$, we obtain:

$$\begin{aligned} Q(\lambda,\lambda^{(t)}) = {} & \sum_S \log \pi_{i_1} P(O,S \mid \lambda^{(t)}) + \\ & \sum_S \left(\sum_{t=1}^{T-1} \log a_{i_t i_{t+1}}\right) P(O,S \mid \lambda^{(t)}) \\ & + \sum_S \left(\sum_{t=1}^{T} \log b_{i_t}(o_t)\right) P(O,S \mid \lambda^{(t)}) \end{aligned} \tag{11}$$

The model parameters π, $\boldsymbol{A}$, and $\boldsymbol{B}$ appear separately in three terms, so they can be maximized independently. The M-step is a constrained optimization problem, which can be solved using the method of Lagrange multipliers. Iterative computation continues until the objective function converges, yielding the optimal model parameters.

However, due to the limited historical defect data of SSCS and the complex relationship between defect types and features, the algorithm often only achieves a local optimum, reducing the model's defect identification accuracy. The initial probability matrix and initial transition probability matrix $\boldsymbol{A}$ have less impact on model training and can be randomly or uniformly initialized using averaging. Yet the initial observation probability matrix $\boldsymbol{B}$ significantly affects the training results [22,23]. Therefore, the particle swarm optimization (PSO) algorithm is introduced to optimize the initial value selection of the observation probability matrix $\boldsymbol{B}$. This helps address the issue of model parameters getting stuck in local optima during training and enhances the model's training speed.

In the PSO algorithm, each bird is regarded as a particle in the solution space [24–26]. There are N particles in total. The position of the i-th particle can be represented as $x_i = (x_{i1}, x_{i2}, \ldots, x_{ir})$, where r denotes the dimensions and matches the dimension of the initial observation probability matrix $\boldsymbol{B}$ in the defect identification model. The velocity of the i-th particle is expressed as $v_i = (v_{i1}, v_{i2}, v_{i3}, \ldots, v_{ir})$. The best position found so far by particle i is $sBest_i = (s_{i1}, s_{i2}, s_{i3}, \ldots, s_{ir})$. The best position discovered by the entire swarm is $sBest = (s_1, s_2, s_3, \ldots, s_r)$. The position update of particle i satisfies the following expressions:

$$v_i(t+1) = c_1 m_1 (sBest_i(t) - x_i(t)) + c_2 m_2 (sBest(t) - x_i(t)) + \omega v_i(t) \tag{12}$$

$$x_i(t+1) = x_i(t) + v_i(t+1) \tag{13}$$

where ω represents the inertial weight, while c_1 and c_2 are the acceleration factors. These factors adjust the step size towards the particle's best position and the global best position found by the swarm. m_1 and m_2 are random numbers between 0 and 1.

The inertia weight mainly affects the displacement size of the current particle's movement, the larger the value taken, the farther the current particle's position is from the previous generation particle's position, and the global search capability of the algorithm will also improve with the increase of the inertia weight. Therefore, through dynamically adjusting the size of the inertia weight factor to improve the global search capability of the PSO algorithm, the inertia weight correction formula is:

$$\begin{cases} dist(t) = \frac{\sqrt{\sum_{i=1}^{N}(x_i(t) - sBest_i(t))}}{N} \\ \omega = \frac{dist(t)}{\max(dist)} \end{cases} \tag{14}$$

where $dist(t)$ represents the average distance from each particle to the global optimal value; $\max(dist)$ represents the maximum value of the historical average distance.

When using the PSO algorithm to optimize the initial observation probability matrix $\boldsymbol{B}$ of the SSCS defect identification model, each possible matrix $\boldsymbol{B}$ is treated as a particle in the solution space. The Forward-Backward algorithm from the defect identification model is selected as the fitness function. The fitness value of each particle is calculated based on the probability $log(P(O|\lambda))$ and updates are made according to these values. The fitness calculation formula is as follows:

$$\begin{cases} log(P(O \mid \lambda)) = log(\sum_{i=1}^{N} \alpha_T(i)) \\ \alpha_t(i) = P(o_1, \cdots, o_t, i_t = q_i \mid \lambda) \\ \alpha_{t+1}(j) = \sum_{i=1}^{N} \alpha_t(i) a_{ij} b_j(o_{t+1}) \end{cases} \tag{15}$$

where $\alpha_t(i)$ represents the forward algorithm.

The optimization process for the initial observation probability matrix $\boldsymbol{B}$ based on PSO is shown in Fig. 3. First, several initial observation probability matrices $\boldsymbol{B}$ are randomly generated. Next, the position and velocity of each particle are updated; the updated particle corresponds to a new observation probability matrix $\boldsymbol{B}$. During each iterative optimization, the individual and global optimal positions of the particle swarm are updated based on the fitness values. The particle's velocity and position are adjusted using equations (12) and (13), and the entire swarm's position is updated according to the new velocity. Iteration continues until the fitness value change meets the threshold or the iteration limit is reached. Finally, the optimal initial observation probability matrix $\boldsymbol{B}$ is output.

Once the initial model parameters $\lambda^{(0)}$ are obtained, the Baum-Welch algorithm is applied to optimize these parameters. In each iteration of the optimization process, the probability $P(O|\lambda^{(n)})$ under the new model parameters is computed. The iteration ceases when the difference between the probabilities of two consecutive iterations falls below a predefined threshold or when the maximum number of iterations is reached, resulting in the defect identification model. During the training of the defect identification model, a separate HMM model must be trained for each defect cause. For N_c types of defect causes, a total of N_c HMM models are trained, denoted as $\{\lambda_n\}_{n=1}^{N_c}$, thereby establishing the SSCS's defect identification model library.

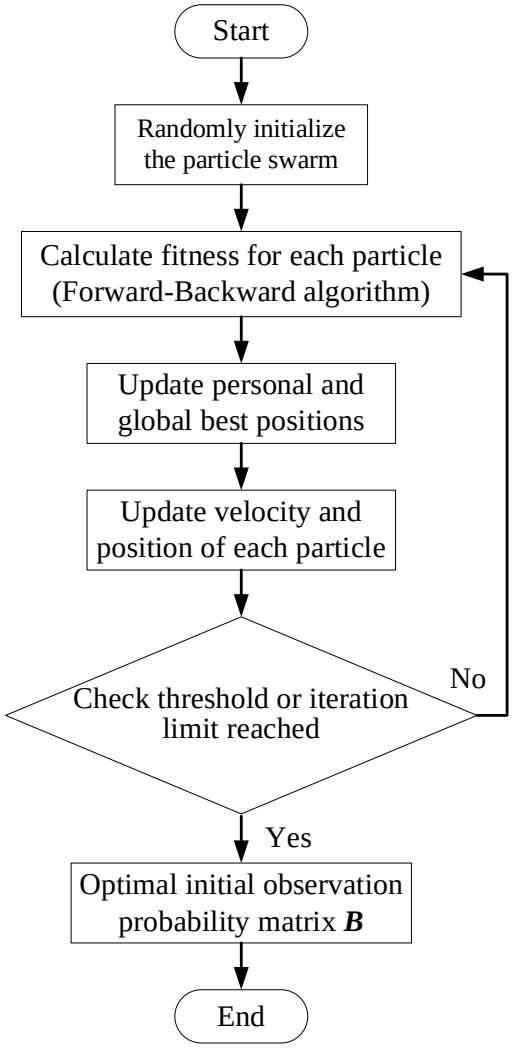

Figure 3. Model parameter optimization process.

Based on the proposed defect identification results, a real-time composite operational risk quantification model is constructed to translate the defect probabilities into dynamic risk values:

$$R_{SSCS} = \sum_{i=1}^{4}(P_i \times \lambda_i \times W_{grid}) \quad (16)$$

where R_{SSCS} is the real-time composite operational risk value of the SSCS; P_i is the posterior probability of the i-th functional link defect output by the SSCS defect identification model in this paper, reflecting the probability of the defect occurring under the current operating state; λ_i is the defect weight factor, characterizing the impact weight of different functional link defects on the correctness of the SSCS device action. Setting limit-exceedance and operation strategy mismatch easily directly lead to disastrous failure to operate or maloperation, and their λ values are set to the highest level; while communication anomaly mainly leads to regional cooperative function degradation, and its λ value is relatively low; W_{grid} is the consequence factor of external power grid topology importance, characterizing the potential power grid load loss that will be caused if a fault occurs in the SSCS node. The model comprehensively considers three dimensions: posterior probability, defect weight factor, and power grid consequence factor. The posterior probability is the defect occurrence probability of each functional link output in real-time by the PSO-HMM model. The defect weight factor characterizes the impact weight of different links on the correctness of the action. For example, setting limit-exceedance and operation strategy mismatch directly threaten the action logic, and the weight is set to the highest level; while communication anomaly mainly affects regional coordination, and the weight is relatively low. The power grid consequence factor combines the current power grid topology importance, characterizing the potential load loss amount that may be caused when a maloperation or failure to operate occurs at this node. Through this model, operation and maintenance personnel can convert the abstract probability distribution into an intuitive risk level, thereby scientifically formulating maintenance priorities and risk control strategies before the defect evolves into a substantial accident.

4. Defect identification process

The defect identification process for SSCS based on PSO-HMM is divided into two parts: offline training and defect identification, as shown in Fig. 4. Measurement errors, data loss, or other anomalies may occur during data collection. To address these issues, data interpolation is used to replace and supplement abnormal or missing data. Additionally, due to the inconsistent metrics and meanings of various feature indicators and their large variations in numerical ranges, nor-malization is performed to eliminate the impact of dimensions on the defect identification model training.

For each defect characteristic vector of the SSCS, preprocessing is performed as follows:

$$x_{i,j}^{'} = \frac{x_{i,j} - x_{j,min}}{xj,min_{j,max}} \quad (17)$$

where $x_{i,j}^{\prime}$ denotes the normalized preprocessing result of the j-th defect characteristic component $x_{i,j}$ in the i-th defect characteristic vector x_i, where n is the number of defect characteristic components in the vector. $x_{j,min}$ and $x_{j,max}$ represent the lower and upper bounds of the j-th defect characteristic component, respectively. The preprocessed i-th defect characteristic vector is denoted as $x_i^{'}$.

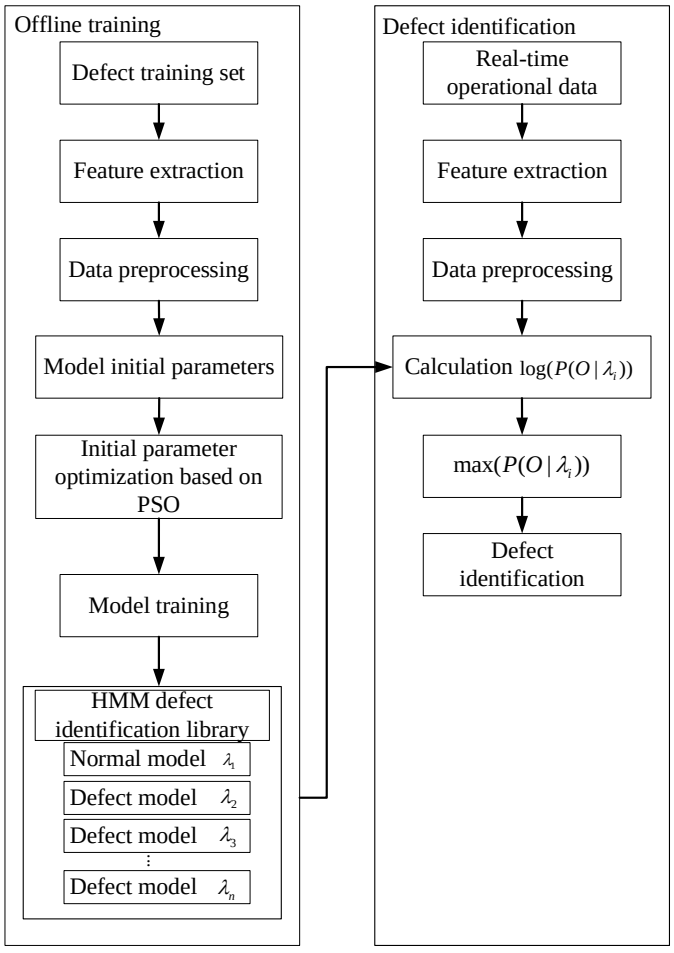

Figure 4. Defect identification process of SSCS based on PSO-HMM.

According to the typical defect characteristics of SSCS, the defects are classified into five categories: normal (no defect), communication anomaly, sampling anomaly, setting limit-

exceedance, and operation strategy mismatch. One-hot encoding is used to represent these defect types. Since the HMM model requires discrete data vectors as input, the preprocessed feature data are clustered using the K-means clustering algorithm [27]. The clustered features are then concatenated in sequence to form the observation data, which is divided into training and testing sets. Subsequently, the HMM is trained using the PSO algorithm and the defect training set to establish a defect identification model library $\{\lambda_n\}_{n=1}^{N_c}$. Finally, real-time operational data to be diagnosed is preprocessed into observation vectors and fed into the model library. The trained defect identification models are used to calculate the log-likelihood probabilities $log(P(O|\lambda))$ of these vectors for each defect model. The defect corresponding to the model with the highest log-likelihood probability is identified as the system defect and output as the result.

5. Evaluation index of defect identification

The accuracy of the SSCS defect identification model is evaluated using recognition accuracy (Acc) and the F1 score. Acc, which represents the accuracy of defect identification in SSCS, is calculated as follows:

$$Acc = \frac{M}{M+N} \tag{18}$$

where *M* represents the number of correct identifications, including both normal and defective conditions. *N* represents the number of incorrect identifications.

The F1 score incorporates two metrics: recall and precision. Recall is the ratio of correctly identified defects to all actual defects in the SSCS. Precision is the ratio of correctly identified defects to all identified defects. The formulas are as follows:

$$\text{Recall} = \frac{TP}{TP+FN} \tag{19}$$

$$\text{Precision} = \frac{TP}{TP+FP} \tag{20}$$

$$\text{F1} = 2 \times \frac{\text{Precision} \times \text{Recall}}{\text{Precision} + \text{Recall}} \tag{21}$$

where *TP* is the number of defect samples correctly identified as defective. *FN* is the number of defective samples wrongly classified as normal. FP is the number of normal samples wrongly classified as defective.

6. Results and discussion

To verify the effectiveness of the proposed method, a regional power grid's SSCS was used as a case study. Data is mainly collected through two categories of approaches: the first is the com-munication and protocol message data obtained through the security information and event management system or the main control center background, including bit error rate, synchroniza-tion time differences, etc.; the second is various physical state data monitoring the operation of SSCS devices in real time through sensors installed on the key components of the SSCS, including board temperature and humidity, current, voltage, etc., and the data is collected through a cen-tralized monitoring system. A total of 2, 500 sample data points covering five types of defect causes were collected. For each defect type, 80% of the data were randomly selected as the training set, and the remaining 20% were used as the test set. The defect identification perfor-mance of the PSO-HMM model was compared with that of the HMM model. The specific num-bers of samples in the training and test sets for each defect cause in the SSCS are detailed in Table 2.

The ten key characteristic quantities listed in Table 1 constitute the observation sequence of the HMM model, while the 5 categories of defects listed in Table 2 constitute the hidden se-quence of the HMM model. Each category of defect corresponds to a specific abnormal varia-tion combination of one or more characteristic quantities. For example, the communication anomaly is mainly manifested as the degradation of time characteristic quantities (bit error rate, synchronization time differences); the sampling anomaly is mainly manifested as the degrada-tion of sampling characteristic quantities (frequency measurement error, switch status acquisition accuracy). Through the learning of the HMM model, the mapping relationship from observation characteristic quantities to SSCS defect types can be automatically established.

Table 2. Defect information and sample number.

Defect causes	Label	Training sample	Test sample
Normal	(0,0,0,0,1)	400	100
Communication anomaly	(0,0,0,1,0)	400	100
Sampling anomaly	(0,0,1,0,0)	400	100
Setting limit-exceedance	(0,1,0,0,0)	400	100
Operation strategy mismatch	(1,0,0,0,0)	400	100

In this paper, the SSCS fault cause identification model is

constructed in Matlab. The model is trained and tested by an experimental platform composed of a CPU of Intel i5 14600 KF, a memory of 32 GB, and a GPU of NVIDIA GeForce 4060Ti. According to the training data set of each defect cause, the HMM model is trained, to obtain the SSCS defect identification models of normal state, communication anomaly, sampling anomaly, setting limit-exceedance, and operation strategy mismatch. During model training, the value of the initial observation probability matrix B has a great influence on the training results of the model, therefore the PSO algorithm is introduced to optimize the model parameter training process. To verify the superiority of the PSO algorithm, it is compared and analyzed with Grey Wolf Optimizer (GWO), Sparrow Search Algorithm (SSA), and no optimization respectively, setting the initial population size to 20, the optimization iteration number to 25, and the fitness function all choose the log-likelihood probability value. The training iteration curves of the 4 algorithms combining various optimization algorithms with Baum-Welch for the communication anomaly HMM model are shown in Fig. 5, and the average training time is shown in Table 3.

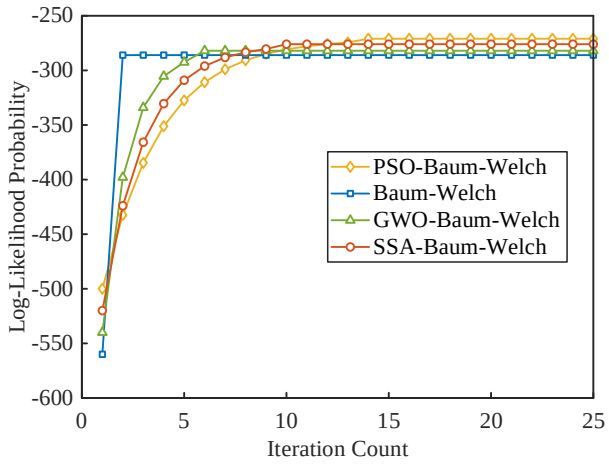

Figure 5. Convergence curves of different optimization algorithms.

From the iteration curves, it can be seen that when adopting the Baum-Welch algorithm to train the model, the convergence speed is relatively fast and it only iterated 2 times. While when adopting the PSO algorithm to train the model, as the iteration times increase, the log-likelihood probability value continuously increases, and it converges after 14 iterations and the log-likelihood probability value is the largest. Adopting the SSA and GWO algorithms iterated 8 times and 11 times respectively, and the convergence values are both lower than the PSO algorithm. The calculation time of the PSO algorithm is longer than the Baum-Welch algorithm, but the model in this paper adopts the strategy of offline training and online identification. After the model training is completed and the SSCS defect identification model library is established, the online identification stage only needs to execute the forward algorithm with extremely low calculation complexity, completely meeting the real-time requirements. Compared with the other 3 methods, PSO-Baum-Welch is less likely to fall into the local optimum, and PSO-Baum-Welch has a faster convergence speed and higher convergence accuracy in the hyperparameter optimization process.

Table 3. The computing time of different optimization algorithms.

Optimize algorithm	Time（s）
Baum-Welch	1.2
PSO-Baum-Welch	4.7
GWO-Baum-Welch	3.5
SSA-Baum-Welch	4.3

Twenty-five samples from each defect cause in the test set were input into the trained HMM model library. Defect identification was based on the maximum output likelihood principle, with results shown in Fig. 6. The identification results show that when the defect identification model trained by PSO-HMM is used to identify defects with test sample data, each type of test sample data achieves the maximum log-likelihood probability value under the corresponding HMM model for defect causes. The results indicate that the identification model trained based on PSO-HMM can effectively identify the defect causes of the safety control system without any errors.

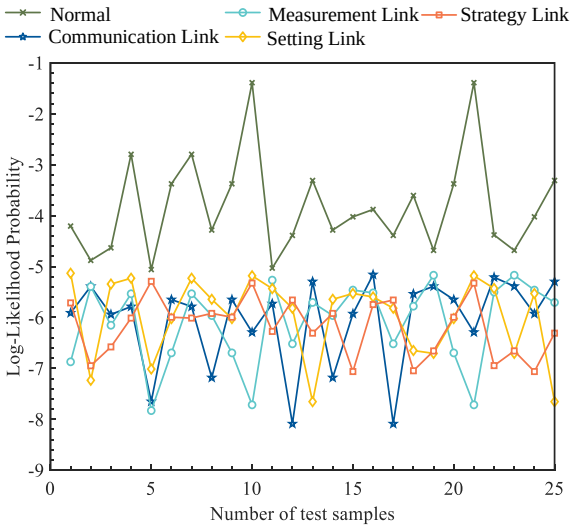

(a)

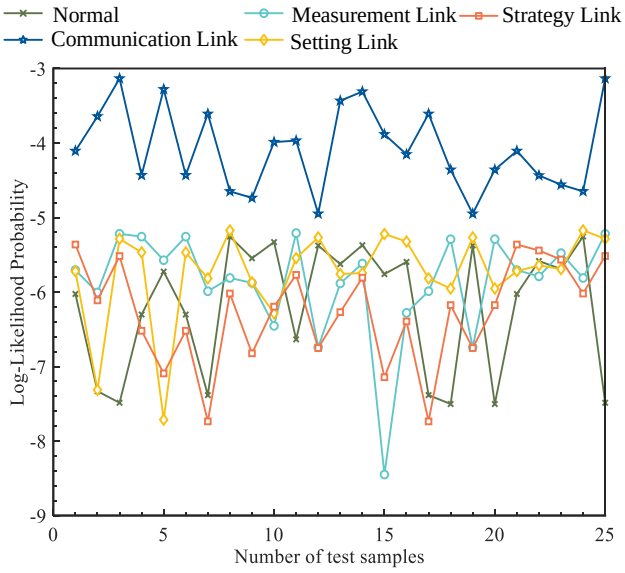

(b)

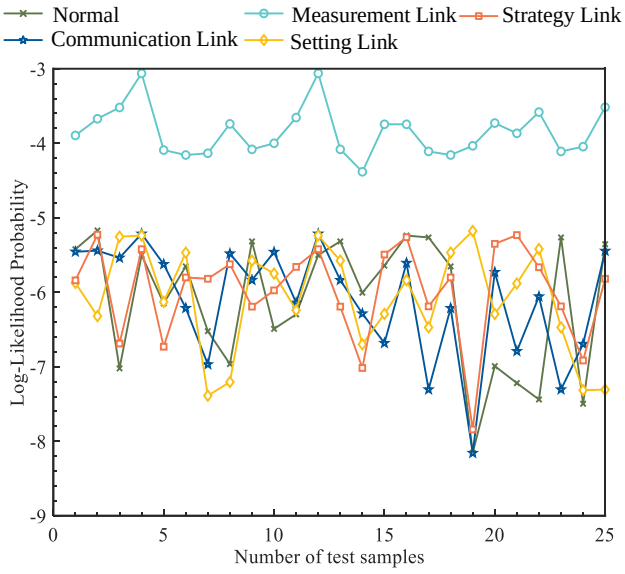

(c)

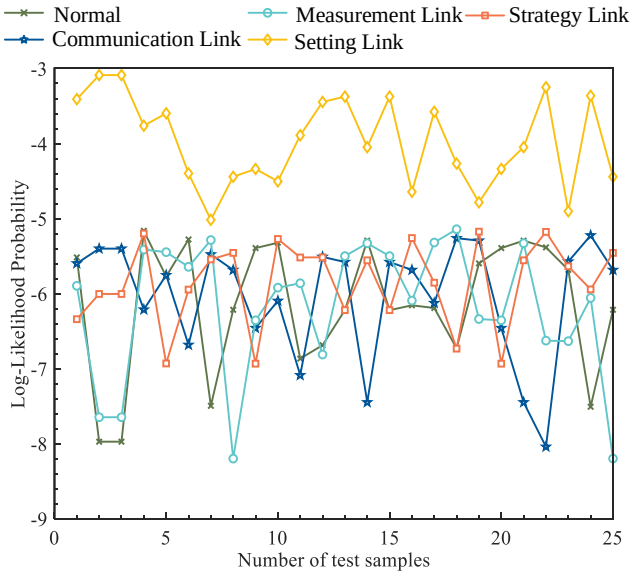

(d)

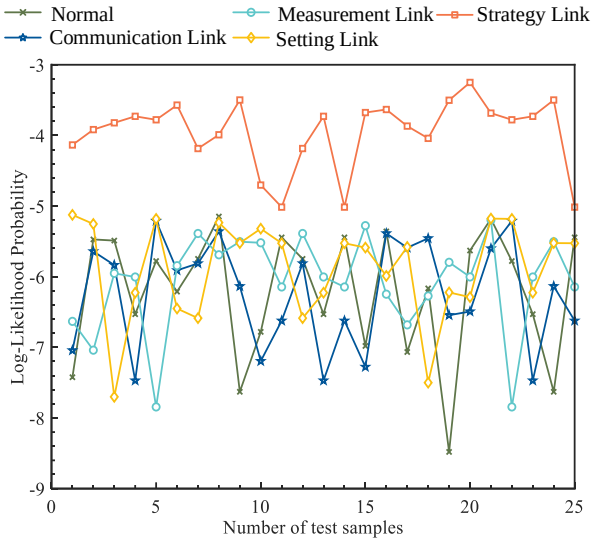

(e)

Figure 6. Defect identification results based on PSO-HMM.

(a) Recognition result of normal condition samples.

(b) Recognition result of communication link defect samples.

(c) Recognition result of measurement link defect samples.

(d) Recognition result of setting link defect samples.

(e) Recognition result of the strategy link defect samples.

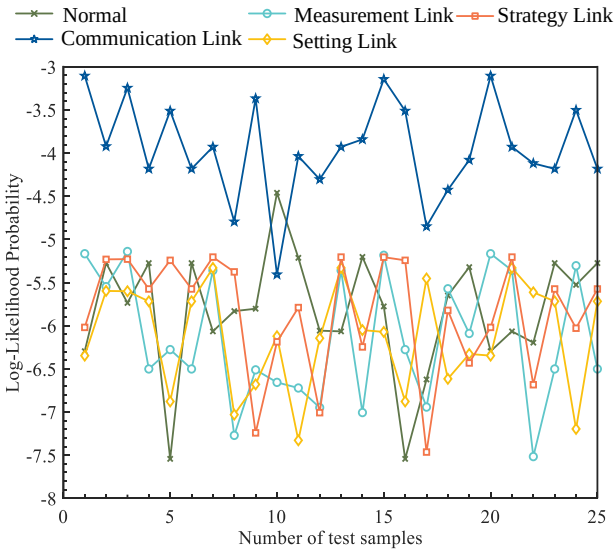

Figure 7. Defect identification results based on HMM.

As shown in Fig. 7, the HMM-based defect identification for the communication link of the SSCS indicates that the 10th group of communication link samples was misclassified as normal. The model accurately identified normal status, measurement link defects, setting link defects, and strategy link defects with 100% accuracy. This validates the effectiveness of the selected defect characteristics. Overall, the results demonstrate that the PSO-HMM-based SSCS defect identification model can effectively extract defect features from

real-time system data and perform accurate defect identification. To compare the defect identification accuracy of the PSO-HMM and HMM models for SSCS, 500 samples were used for testing. The results in Table 4 show that the PSO-HMM model has higher accuracy across all defect categories. For normal conditions, the accuracy improved by 10%; for communication faults, by 7%; for sampling faults, by 8%; for setting limit-exceedances, by 8%; and for operation strategy mismatches, by 11%. The overall accuracy of the PSO-HMM model reached 92.2%, which is an 8.8% improvement over the traditional HMM model. This indicates that the PSO-HMM model effectively enhances defect identification and can be effectively applied to SSCS.

Table 4. Recognition accuracy of different models.

Defect causes	Recognition accuracy	
	HMM	PSO-HMM
Normal	86%	96%
Communication anomaly	84%	91%
Sampling anomaly	81%	89%
Setting limit-exceedance	85%	93%
Operation strategy mismatch	81%	92%
Overall	83.4%	92.2%

7. Conclusion

At present, the SSCS has been increasingly integrated into the control and operation of modern power grids, further contributing to the structural complexity of the grid. As an essential compo-nent of grid control, maintaining the proper operational state of the SSCS is of great importance. However, the SSCS faces challenges such as limited historical defect data, complex coupling re-lationships among devices, and diverse defect characteristics. These issues make it difficult to effectively extract useful information from characteristic parameters, resulting in the absence of an effective defect identification approach for the SSCS. To address this, this paper establishes a SSCS defect identification model based on PSO-HMM and proposes a corresponding identifica-tion method. By inputting real-time SSCS features into the identification model, it can identify potential defects in communication, measurement, setting, and strategy links. This enables re-al-time monitoring of system operation and provides a scientific basis for condition-based maintenance, playing a significant role in ensuring grid safety and stability.

To expand the scope of defect identification, future work will consider integrating device self-checking data and alarm text analysis. Addressing the computational bottlenecks and the lack of a global optimality guarantee in current PSO-based HMM training, researchers will ex-plore adaptive optimization algorithms to improve training efficiency and search performance. Beyond identification, the focus will shift toward predicting SSCS degradation trends. By con-tinuously monitoring the evolution trajectory of log-likelihood probabilities for various states, the system's health degradation rate can be quantified. This transition from reactive diagnosis to proactive maintenance provides a scientific basis for issuing early warnings before hardware failures occur.

Acknowledgment

I express my gratitude to the anonymous reviewers for their comments and suggestions, which have greatly helped me to improve the content, quality, organization, and presentation of this work. This work was supported by the State Grid Corporation of China Technology Project (SGSW0000DKJS2400081).

References

1. Zhao L, Li X, Ni M, Li T, Cheng Y. Review and prospect of hidden failure: protection system and security and stability control system. *Journal of Modern Power Systems and Clean Energy* 2019; 7(6): 1735-43. https://doi.org/10.1007/s40565-015-0128-9.
2. Ren H, Mi Z. Power System Fault diagnosis modeling techniques based on encoded petri nets. *2006 IEEE Power Engineering Society General Meeting* 2006; https://doi.org/10.1109/pes.2006.1709100.
3. Deng B, Wen Y, Jiang X. Total transfer capability assessment of HVDC tie‐lines in asynchronous grids. *IET Generation, Transmission & Distribution* 2021; 15(20): 2872-82. https://doi.org/10.1049/gtd2.12223.
4. Ren C, Niu S, Ke X, Huo C, Lu H. Optimization research and realization of UHVDC security control system in northwest power grid. *High Voltage Engineering* 2020; 46(9): 3229-3237. https://doi.org/10.13336/j.1003-6520.hve.20200302012.
5. Bai S, Li J, Xu S, Xu S, Zhu Y, Zhao X. Research and Development of Real-Time Fast Security and Stability Control System for Large

Power Grid. *Process Automation Instrumentation* 2021; 42(8): 77-83. https://doi.org/10.16086/j.cnki.issn1000-0380.2020120062.

6. Massaoudi MS, Abu-Rub H, Ghrayeb A. Navigating the landscape of deep reinforcement learning for Power System Stability Control: A review. *IEEE Access* 2023; 11: 134298-317. https://doi.org/10.1109/access.2023.3337118.
7. Tavakoli M, Nafar M. Human reliability analysis in maintenance team of Power Transmission System Protection. *Protection and Control of Modern Power Systems* 2020; 25: 5(1). https://doi.org/10.1186/s41601-020-00176-6.
8. Zhou H, Shi H, Zeng L, Wang F, Ouyang Y. Fault diagnosis of an intelligent substation secondary device based on a relational hypergraph-enhanced transformer. *Power System Protection and Control* 2024; 52(12): 123-132. https://doi.org/10.19783/j.cnki.pspc.231475.
9. Yin X, Zhang W, Lu Z, Hou F, Wang L. Research on fault diagnosis method for secondary equipment of intelligent substation. *Electrical Measurement & Instrumentation* 2020; 57(3): 39-45. https://doi.org/10.19753/j.issn1001-1390.2020.03.007.
10. Yan M, Yang Y, Zhao F. A data stream anomaly detection method based on an improved ocsvm smart substation. *Power System Protection and Control* 2022; 50(6): 100-106. https://doi.org/10.19783/j.cnki.pspc.210946.
11. Kan J, Dong X, Wang M, Xia H. Dynamic reliability evaluation method of power grid security andstability control system based on Markov chain Monte Carlo. *Electric Power Engineering Technology* 2024; 43: 23-31. https://doi.org/10.12158/j.2096-3203.2024.03.003.
12. Yu R, Zhong L, Chen B, Xiong J, Zhu K, Zhou. Online state evaluation method of stability control system considering index classification. *Advanced Technology of Electrical Engineering and Energy* 2023; 42: 79-88. https://doi.org/10.12067/ATEEE2202013.
13. Zhao L, Li X, Ni M, Cheng Y. Review and prospect of research on hidden failures of protection system and security and stability control system. *Automation of Electric Power Systems* 2021; 38: 128-135. https://doi.org/10.7500/AEPS20140128004.
14. Luo J, Dong X, Cui X, Li D, Li H, Li X, Wang J. Discussion on reliability of large scale security and stability control system. *Power System Protection and Control* 2014; 38: 128-135. https://doi.org/10.7667/PSPC170595.
15. Wu D, Tang X, Li P, Yang Z, Wen B, Li H. State monitoring technology of substation relay protection device based on deep neural network. *Power System Protection and Control* 2020; 48: 81-85. https://doi.org/10.19783/j.cnki.pspc.190516.
16. Jiang, H., Xiong J, Xiang Z, Wang J, Chen Y. Correlation analysis of smart grid safety and stability control device defects based on improved apriori algorithm. *Electrical Measurement & Instrumentation* 2024; 61: 195-20. https://doi.org/10.19753/j.issn1001-1390.2024.10.026.
17. Han W, Duan W, Du X, Yao F, Ma W, Liu L. Fault diagnosis method for operational security control system based on digital twins. *Electric Power* 2023; 56: 121-127. https://doi.org/10.11930/j.issn.1004-9649.202306047.
18. Ouyang J, Zhang A, Jiang H, Xiong J, Zhu K. Fault diagnosis method of power grid security and stability control system based on deep belief network. *Electrical Measurement & Instrumentation* 2024; 61: 1-6. https://doi.org/10.19753/j.issn1001-1390.2024.07.001.
19. Jiang H, Xiong J, Chen Y, Chen B, Feng K, Liu P. Modeling method for hidden faults of stability control system based on Markov state space method. *Advanced Technology of Electrical Engineering and Energy* 2023; 42, 39-47. https://doi.org/10.12067/ATEEE2201016.
20. Qi D, Dirk S. A review of hmm-based approaches of driving behaviors recognition and prediction. *IEEE Transactions on Intelligent Vehicles* 2021; 7: 21-31. https://doi.org/10.1109/tiv.2021.3065933.
21. Li Z, Fang H, Huang M, Wei Y, Zhang L. Data-driven bearing fault identification using improved hidden Markov model and self-organizing map. *Computers & Industrial Engineering* 2018; 1: 116: 37-46. https://doi.org/10.1016/j.cie.2017.12.002.
22. Song Y, Zhao P, Zhou Q, Li T. Chain failure prediction based on time-varying hidden markov model. *Electrical Measurement & Instrumentation* 2023; 60: 146-153. https://doi.org/10.19753/j.issn1001-1390.2023.01.021.
23. Wu L, Feng Z, Zhu X. Pipeline blocking state assessment based on optimized vmd and continuous hidden markov model. *Journal of Vibration and Shock* 2020; 39: 214-222+233. https://doi.org/10.13465/j.cnki.jvs.2020.22.029.
24. Mien V, Hee-Juu K. Bearing defect classification based on individual wavelet local fisher discriminant analysis with particle swarm optimization. *IEEE Transactions on Industrial Informatics* 2015; 12: 124-135. https://doi.org/10.1109/TII.2015.2500098.
25. Wang Y, Hao Y, Wang L, Dang X, Jiang L, Zhang Y, Xiao Q. Multi-objective optimal dispatching for multi-energy microgrid based on im proved particle swarm optimization algorithm. *Electrical Measurement & Instrumentation* 2023; 60: 29-36+59. https://doi.org/10.19753/j.issn1001-1390.2023.11.004.
26. Song L, Liang Q, Chen H, Hu H, Luo Y, Luo Y. A new approach to optimize svm for insulator state identification based on improved PSO algorithm. *Sensors* 2022; 23: 272. https://doi.org/10.3390/s23010272.

27. Yu S, Chu S, Wang C, Chan Y, Chang T. Two improved K-means algorithms. *Applied Soft Computing* 2018; 68: 747-55. https://doi.org/10.1016/j.asoc.2017.08.032.

Nomenclature

Abbreviations	
SSCS	Security and stability control system
HMM	Hidden Markov Model
PSO	Particle Swarm Optimization
ACC	Accuracy